AMERICAN SOCIETY FOR MICROBIOLOGY | Antimicrobial Agents and Chemotherapy®

SUSCEPTIBILITY

A Cationic Polymer That Shows High Antifungal Activity against Diverse Human Pathogens

Leslie A. Rank,[a] Naomi M. Walsh,[b] Runhui Liu,[a]* Fang Yun Lim,[c] Jin Woo Bok,[c] Mingwei Huang,[b] Nancy P. Keller,[c] Samuel H. Gellman,[a] Christina M. Hull[b,c]

Department of Chemistry, University of Wisconsin–Madison,[a] and Department of Biomolecular Chemistry[b] and Department of Medical Microbiology and Immunology,[c] School of Medicine and Public Health, University of Wisconsin–Madison, Madison, Wisconsin, USA

ABSTRACT Invasive fungal diseases are generally difficult to treat and often fatal. The therapeutic agents available to treat fungi are limited, and there is a critical need for new agents to combat these deadly infections. Antifungal compound development has been hindered by the challenge of creating agents that are highly active against fungal pathogens but not toxic to the host. Host defense peptides (HDPs) are produced by eukaryotes as a component of the innate immune response to pathogens and have served as inspiration for the development of many new antibacterial compounds. HDP mimics, however, have largely failed to exhibit potent and selective antifungal activity. Here, we present an HDP-like nylon-3 copolymer that is effective against diverse fungi while displaying only mild to moderate toxicity toward mammalian cells. This polymer is active on its own and in synergy with existing antifungal drugs against multiple species of *Candida* and *Cryptococcus*, reaching levels of efficacy comparable to those of the clinical agents amphotericin B and fluconazole in some cases. In addition, the polymer acts synergistically with azoles against different species of *Aspergillus*, including some azole-resistant strains. These findings indicate that nylon-3 polymers are a promising lead for development of new antifungal therapeutic strategies.

KEYWORDS antifungal agents, antimicrobial peptides, broad spectrum, drug synergy, fungal pathogenesis, nylon-3 polymers

Host defense peptides (HDPs) are part of the eukaryotic innate immune response to invasion by bacteria, fungi, viruses, and protozoa (1, 2), and these peptides have been recognized as potential sources of antimicrobial agents (2). HDPs have diverse amino acid compositions and sizes; many examples are rich in cationic and hydrophobic residues. Some HDPs target fungi in preference to bacteria, while others are active against both bacteria and fungi (3). Among antifungal HDPs, some are more active against filamentous fungi than against yeast, such as plant heavin-type peptides and hairpinins, while others have the opposite selectivity, such as the histatins and mammalian defensins (3). Although antifungal mechanisms of action remain unresolved, there is evidence to suggest that fungi may be attacked via binding to the cell wall, membrane permeabilization, and/or interactions with intracellular targets to generate reactive oxygen species and ultimately cause apoptosis (1, 3–6). Amphipathicity (i.e., the presence of both cationic moieties and hydrophobic moieties) is hypothesized to be essential for microbial membrane permeabilization by HDPs.

Efforts to develop HDPs as clinical antimicrobial agents, unsuccessful thus far, have been hampered by the high cost of production, susceptibility to proteolysis *in vivo*, delivery challenges, and limited antibacterial potency, among other problems (2, 7). A subset of these problems, including production cost and enzymatic degradation, might

Received 31 January 2017 **Returned for modification** 7 March 2017 **Accepted** 18 July 2017

Accepted manuscript posted online 24 July 2017

Citation Rank LA, Walsh NM, Liu R, Lim FY, Bok JW, Huang M, Keller NP, Gellman SH, Hull CM. 2017. A cationic polymer that shows high antifungal activity against diverse human pathogens. Antimicrob Agents Chemother 61:e00204-17. https://doi.org/10.1128/AAC.00204-17.

Address correspondence to Nancy P. Keller, npkeller@wisc.edu, Samuel H. Gellman, gellman@chem.wisc.edu, or Christina M. Hull, cmhull@wisc.edu.

* Present address: Runhui Liu, State Key Laboratory of Bioreactor Engineering, School of Materials Science and Engineering, East China University of Science and Technology, Shanghai, China.

L.A.R., N.M.W., R.L., and F.Y.L. contributed equally to this work.

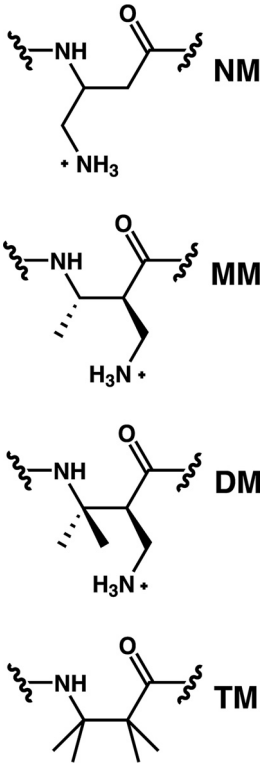

FIG 1 Subunits in the nylon-3 polymers discussed here. The cationic NM (no methyl), MM (monomethyl), and DM (dimethyl) subunits are derived from racemic precursors. The precursor to the hydrophobic TM (tetramethyl) subunit is achiral.

be addressed by use of synthetic polymers that mimic key functional properties of HDPs. The possibility that the biological activity profiles of sequence-specific antibacterial peptides could be reproduced by sequence-random copolymers was first explored over a decade ago (8–10).

Polymers in the nylon-3 family have been particularly well studied as antimicrobial agents. These materials are generated via ring-opening polymerization of β-lactams, and β-lactams bearing a wide variety of side chains can be conveniently synthesized on large scale (11, 12). The nylon-3 subunit is a β-amino acid residue; therefore, these polymers have a backbone featuring periodic secondary amide groups that is reminiscent of the protein backbone but is impervious to degradation by natural proteases (which cleave α-amino bonds). This protein-like, hydrophilic backbone is expected to promote both biocompatibility and stability of nylon-3 materials. Initial studies identified binary nylon-3 copolymers containing both hydrophobic and cationic subunits that displayed potent antibacterial activity but little or no hemolytic activity against human red blood cells (11, 12). More recently, nylon-3 polymers with selective antifungal activity have been described. The first such examples were homopolymers containing the cationic NM (no methyl) subunit (Fig. 1), which were active against the K1 strain of *Candida albicans* (13). Subsequent efforts to achieve activity against other fungal pathogens, such as species of *Cryptococcus* and *Aspergillus*, revealed that incorporation of a hydrophobic subunit was necessary for antifungal activity (14).

In an ongoing effort to improve antifungal activities among nylon-3 materials, we have now examined new binary copolymers containing the hydrophobic TM (tetramethyl) subunit paired with either the MM (monomethyl) or DM (dimethyl) cationic unit (Fig. 1). Preliminary studies (see supplemental material) focused our attention on the MM-TM copolymer that is the subject of the studies reported below. This copolymer displays activity against fungi from the three genera that cause the majority of fungus-related deaths worldwide, *Cryptococcus*, *Candida*, and *Aspergillus* (15). These

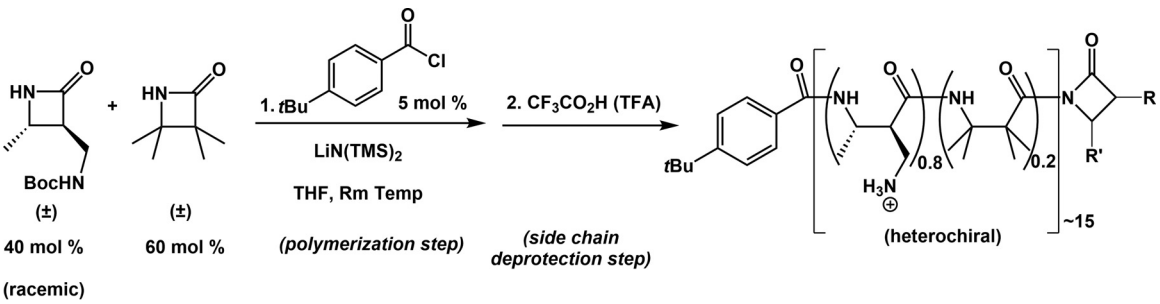

FIG 2 Nylon-3 copolymers are synthesized by the anionic-ring-opening polymerization (AROP) of β-lactams. The MM-TM copolymer was synthesized by the AROP of a cationic subunit and a hydrophobic subunit in tetrahydrofuran (THF). MMβ (monomethyl; racemic) and TMβ (tetramethyl) were mixed in a 2:3 molar ratio. 4-*tert*-Butylbenzoyl chloride (5 mol%, which is intended to produce an average chain length of 20 subunits) was used as the reaction initiator, and lithium bis(trimethylsilyl)amide [$LiN(TMS)_2$] was used as the base. After polymerization was complete, deprotection was carried out with trifluoroacetic acid (TFA) at room temperature (Rm Temp). The resulting MM-TM copolymer was found to contain roughly 80 mol% MM and 20 mol% TM, with a 15-mer average chain length (molecular mass of 3,300 g/mol).

fungi cause invasive disease in both healthy and immunocompromised individuals, and they exhibit different susceptibilities to current antifungal drugs. The inadequacy of current therapeutic options contributes to high morbidity and mortality from invasive fungal diseases. Here, we characterize antifungal activities of the MM-TM copolymer alone and in combination with current antifungal drugs and evaluate polymer lytic activity toward mammalian cells.

RESULTS

Nylon-3 copolymer synthesis. The MM-TM copolymer was prepared from a 2:3 molar mixture of the β-lactams MMβ (monomethyl; racemic) and TMβ (Fig. 2). 4-*tert*-Butylbenzoyl chloride was included to serve as the *in situ* precursor for the N-acyl-β-lactam species that acts as a coinitiator of the polymerization reaction. A coinitiator is required for control of average chain length in these reactions, and average chain lengths of <30 subunits have been shown previously to favor lower hemolytic activity (12). We used 5 mol% 4-*tert*-butylbenzoyl chloride relative to the total amount of β-lactam, which is predicted to lead to a 20-mer average chain length. Unlike traditional chemical syntheses, which are intended to provide material that contains only one type of molecule, nylon-3 polymer samples contain a diverse population of molecules that vary in composition, subunit sequence, subunit stereochemistry, and chain length. Therefore, we assessed the consistency of the polymerization process by comparing MM-TM copolymer samples generated via independent reactions.

Synthetic polymer samples were characterized via two measurements, ^{1}H nuclear magnetic resonance (^{1}H NMR) and gel permeation chromatography (GPC). The NMR-based compositional analysis provided very consistent results for eight independently synthesized samples of the MM-TM copolymer (Table 1), showing similar subunit proportions in each sample (~80 mol% MM and ~20 mol% TM). However, this composition does not mirror the 2:3 ratio of MMβ and TMβ employed for the polymerization reactions; the difference between the initial β-lactam ratio and the final subunit ratio presumably reflects differences in β-lactam reactivity (i.e., TMβ is less reactive than MMβ).

To determine the average chain length, or degree of polymerization (Dp), of the eight MM-TM samples, we conducted GPC analysis of protected copolymers (i.e., samples in which the side chain amino groups of MM subunits retain the *tert*-butyloxycarbonyl [Boc] protecting group that is present in MMβ). We also conducted NMR analysis of deprotected copolymers. These analyses indicated average chain lengths of 15 ± 1 (Dp determined by NMR [Dp_{NMR}]) and 19 ± 4 subunits (Dp determined by GPC [Dp_{GPC}]) We then used the NMR-based chain length (15 units) to calculate the average molecular mass of the polymers. The eight polymerization reactions provided samples characterized by relatively similar average molecular mass values, with an overall average molecular mass of 3,300 g/mol ± 390 g/mol (Table 1).

TABLE 1 MM-TM nylon-3 copolymer characterization[a]

Batch	GPC characterization				NMR characterization	
	D_{GPC}[d]	Mn_{GPC}[e]	Dp_{GPC}[f]	Dp_{NMR}[g]	Observed subunit ratio (MM:TM)[h]	Mn_{NMR}[i]
1[b]	1.27	4,461	22	15	80:20	3,280
2[b]	1.18	4,529	22	14	79:21	3,058
3[b]	1.20	3,723	18	14	79:21	3,723
4[b]	1.19	4,715	23	16	81:19	3,504
5[c]	1.24	2,195	11	12	75:25	2,596
6[b]	1.16	4,262	21	15	80:20	3,280
7[b]	1.21	4,168	20	15	80:20	3,280
8[b]	1.21	3,291	15	13	77:33	3,824

[a]The average bulk molecular mass was 3,300 g/mol ± 390 g/mol.
[b]Side chain-protected polymer characterization by gel permeation chromatography (GPC) using *N*,*N*-dimethylacetamide (DMAc) as the mobile phase.
[c]Side chain-protected polymer characterization by GPC using tetrahydrofuran (THF) as the mobile phase.
[d]D_{GPC}, dispersity index by GPC.
[e]Mn_{GPC}, number-average molecular mass of side chain-protected polymers.
[f]Dp_{GPC}, degree of polymerization or average polymer chain length as calculated from Mn_{GPC} using the subunit ratios determined from nuclear magnetic resonance (NMR) analysis.
[g]Dp_{NMR}, degree of polymerization or average polymer chain length as calculated by NMR integrations based on end group analysis, i.e., the assumption that each chain contains only one *tert*-butyl benzoyl group.
[h]The MM:TM subunit ratio for each polymer sample was calculated from NMR integrations.
[i]Mn_{NMR}, the number-average molecular mass of side chain-deprotected polymers, based on NMR-calculated subunit ratios.

The MM-TM copolymer shows activity against multiple species of *Candida*. We used the CLSI M27-A3 broth microdilution method (17) to determine the MIC (MIC that inhibits 100% growth [MIC_{100}]) values of the MM-TM copolymer against four strains of *Candida albicans* and one strain of *Candida lusitaniae* (Table 2). Three of the four strains of *C. albicans* tested were drug-resistant isolates: K1 (fluconazole [FLC] resistant), Gu5 (FLC resistant), and E4 (FLC and amphotericin B [AMB] resistant). MIC_{100} assays were performed for all *Candida* strains with suspensions of 1.25×10^3 cells/ml at 35°C. Synergy assays were conducted with suspensions of 1.25×10^5 cells/ml at 30°C.

The MM-TM copolymer showed moderate activity against all four strains of *C. albicans* (MIC_{100} values of 5 to 9 μM [5 to 30 μg/ml]; Table 3). Comparable activity was observed against *C. lusitaniae* (CL3), with an MIC_{100} of 1.4 μM (4.7 μg/ml). As benchmarks, MIC_{100} for the *Candida* test strains were determined using amphotericin B and fluconazole; the results of these control studies were consistent with previous reports (21–23). Thus, AMB manifested MIC_{100}s of $<$1.7 to 2.2 μM ($<$1.6 to 2.0 μg/ml) except for strain E4, which is resistant to AMB with an MIC_{100} of 6.8 μM (6.3 μg/ml) (21). FLC was very active in two cases (MIC_{100} and MIC_{50} of $<$5.2 μM [$<$1.6 μg/ml]) but not against the resistant strains (MIC_{100} of $>$600 μM [$>$200 μg/ml]) (Table 3) (22, 23). Interestingly, the AMB- and FLC-resistant strains of *C. albicans* showed no differences in sensitivity to the copolymer relative to sensitive strains, which suggests that the mechanism of antifungal action for MM-TM differs from that for AMB or FLC.

To test whether the MM-TM copolymer could act synergistically with FLC, which is commonly used to treat candidiasis, we exposed two *Candida* strains to MM-TM and FLC at the same time. Checkerboard tests were used to determine the fractional inhibitory concentrations (FIC) of the combination of FLC and MM-TM copolymer against the FLC-sensitive strain SC5314 and FLC-resistant strain K1. Assays were performed at 30°C and ambient levels of CO_2 to maintain the yeast morphology of the strains. The data indicated that there was no synergism between MM-TM and FLC against strain SC5314 ($\sum$FIC index value of 1.0) (Table 4), a situation in which FLC alone is very active. In contrast, FLC and MM-TM in combination appeared synergistic ($\sum$FIC index value of 0.08) against the FLC-resistant K1 strain (Table 4). FLC MIC_{100} values against the K1 strain in combination with copolymer decreased dramatically, resulting in a $\geq$100-fold improvement in antifungal activity relative to the MIC_{100} of FLC as a single agent.

TABLE 2 Strains used in this study

Species	Strain	Origin	Drug resistance[a]	Feature(s) or marker(s)	Source
Candida spp.					
C. albicans	SC5314	Clinical			ATCC (ATCC MYA-2876)
C. lusitaniae	CL3	Clinical		*MTLα*	ATCC (ATCC 42720)
C. albicans	K1	Clinical	Fluconazole*		Gift from Bruce Klein lab, UW-Madison[b]
C. albicans	Gu5	Clinical (Germany)	Fluconazole*		ATCC (ATCC MYA-574)
C. albicans	E4	Clinical	Polyene antibiotics* (amphotericin B)		ATCC (ATCC 38248)
Cryptococcus spp.					
C. neoformans	H99	Clinical (NY, US)		Serotype A; *MATα*	ATCC (ATCC 208821)
C. neoformans	B3501	Single progeny from cross ATCC 28957 × ATCC 28958		Serotype D; *MATα*	ATCC (ATCC 3487)
C. neoformans	JEC21	Derived from B-3501 and B-3502		Serotype D; *MATα*	ATCC (ATCC 96910)
C. neoformans	C21F3	Derived from JEC 21 (ATCC 96910)	Rapamycin* and FK506*	Serotype D; *MATα*; does not express FKBP12	ATCC (ATCC MYA-737)
C. gattii	WM276	Environmental (Sydney, Australia)		Serotype B; *MATα*	ATCC (ATCC 4071)
C. gatti	C751/PNG9	Clinical (Papua New Guinea)		Serotype B; *MATα*	Gift from Dee Carter lab, University of Sydney
Aspergillus spp.					
A. fumigatus	AF293	Clinical (UK)			ATCC (ATCC MYA-4609)
A. fumigatus	CEA10	Clinical			Keller laboratory
A. fumigatus	F11628	Clinical (Liverpool, UK)	Azole*	Cyp51A mutation G138C	Regional Mycology Laboratory Manchester; gift from David Denning; Keller laboratory (26)
A. fumigatus	F16216	Clinical (Northampton, UK)	Azole*	Cyp51A mutation L98H + TR	Regional Mycology Laboratory Manchester; gift from David Denning; Keller laboratory (26)
A. terreus	NIH2624				Keller laboratory

[a]Drug resistance as reported by the ATCC is indicated by an asterisk.
[b]UW-Madison, University of Wisconsin–Madison.

TABLE 3 MIC results for MM-TM against *Candida* spp.[a]

Isolate	MM-TM[b] MIC_{100} (μM) ($\mu g/ml$)	AMB[c] MIC_{100} (μM) ($\mu g/ml$)	FLC[d] MIC_{100} (μM) ($\mu g/ml$)	FLC[d] MIC_{50} (μM) ($\mu g/ml$)
C. albicans SC5314	4.8 (*15.7*)	<1.7 (<*1.6*)	<5.2 (<*1.6*)	<5.2 (<*1.6*)
C. lusitaniae CL3	1.4 (*4.7*)	<1.7 (<*1.6*)	<5.2 (<*1.6*)	<5.2 (<*1.6*)
C. albicans K1	7.6 (*25*)	<1.7 (<*1.6*)	>650 (>*200*)	<5.2 (<*1.6*)
C. albicans Gu5	9.5 (*31.3*)	2.2 (*2.0*)	>650 (>*200*)	326 (*100*)
C. albicans E4	4.2 (*14.0*)	6.8 (*6.3*)	>650 (>*200*)	<5.2 (<*1.6*)

[a]MIC_{100} or MIC_{50} results by broth microdilution. The inoculum density was 1.25×10^3 cells/ml, and the isolates were incubated for 24 h at 35°C. Each experiment was repeated in duplicate on separate days in at least two different trial experiments. The MIC_{100} (MIC that inhibits 100% growth) or MIC_{50} (MIC that inhibits 50% growth) values are given in micromolar concentrations. The italic values within parentheses are given in micrograms per milliliter.
[b]The average molecular mass of the MM-TM copolymer used for molarity conversion is 3,300 g/mol.
[c]AMB, amphotericin B (molecular mass, 924.091 g/mol).
[d]FLC, fluconazole (molecular mass, 306.271 g/mol).

The MM-TM copolymer shows activity against multiple species of *Cryptococcus*. We determined MIC_{100} values for MM-TM against four strains of *Cryptococcus neoformans* and two strains of *Cryptococcus gattii* using the CLSI M27-A3 broth microdilution method (17) (Table 2). The MIC_{100} values of <1 μM (<3 μg/ml) were measured for the MM-TM copolymer against all *Cryptococcus* spp. tested (Table 5). For comparison of MM-TM with currently used antifungal drugs, we measured MIC_{100} values for the *Cryptococcus* test strains using AMB and FLC. All results were consistent with previous reports: MIC_{100} of ~1 μM (~1 μg/ml) for AMB and MIC_{100} and MIC_{50} of ≤10 μM (≤3.1 μg/ml) for FLC (Table 5) (24).

To test whether the MM-TM copolymer could act synergistically with AMB, which is commonly used to treat cryptococcosis, we exposed the virulent type strain (H99) to MM-TM and AMB at the same time. Checkerboard tests were used to determine the fractional inhibitory concentrations of the combination of AMB and MM-TM copolymer. AMB and MM-TM acted synergistically against strain H99 (∑FIC index value of 0.08), decreasing the MIC_{100} of AMB by >10-fold, and this synergy was fungicidal (Table 6).

The MM-TM copolymer shows synergism with azole drugs against *Aspergillus* spp. We determined the MIC_{100} values for MM-TM against four strains of *Aspergillus fumigatus* and one strain of *Aspergillus terreus* (Table 7). In contrast to our findings with *Candida* spp. and *Cryptococcus* spp., we found that the MM-TM copolymer was not

TABLE 4 Synergy results with FLC and MM-TM against *Candida albicans* isolates[a]

Isolate	Test agent	MIC_{100} of test agent (μM) ($\mu g/ml$)[b] Alone[c]	Combination[d]	∑FIC index[e]	FIC interpretation
SC5314	MM-TM	20 (*67*)	<0.02 (<*005*)[f]	1.00	Indifferent
	FLC	<1.0 (<*0.3*)[f]	<1.0 (<*0.3*)[f]		
K1	MM-TM	30 (*100*)	2.6 (*8.4*)	0.08	Synergistic
	FLC	>160 (>*50*)[f]	<1.3 (<*0.4*)[f]		

[a]The inoculum density was 1.25×10^5 cells/ml, and the isolates were incubated for 48 h at 30°C. The inoculum density was increased for synergy studies 100-fold to 1.25×10^5 cells/ml relative to MIC studies to ensure there was sufficient inoculum for fungicidal testing. Each experiment was repeated in duplicate on separate days in at least two different trial experiments.
[b]The MIC_{100} of the test agent is shown in micromolar. The italic values within parentheses are the MIC_{100} values in micrograms per milliliter.
[c]MIC as determined by OD_{600} measurements after 48 h for the test agent alone.
[d]MIC as determined by OD_{600} measurements after 48 h for test agents incubated with *Candida* in combination.
[e]Fractional inhibitory concentration (FIC).
[f]The high off-scale MIC value, >163.5 μM, was converted to the next highest concentration, 327 μM, for calculation of the FIC index. The low off-scale MIC values were converted to the next lowest concentration (onefold serial dilution) for calculation of the FIC index.

TABLE 5 MIC results for MM-TM against *Cryptococcus* spp.[a]

Isolate	MM-TM[b] MIC_{100} (μM) (μg/ml)	AMB[c] MIC_{100} (μM) (μg/ml)	FLC[d] MIC_{100} (μM) (μg/ml)	FLC[d] MIC_{50} (μM) (μg/ml)
C. neoformans isolates				
JEC21	0.5 (*1.6*)	0.2 (*0.2*)	5.2 (*1.6*)	0.3 (*0.1*)
B3501	0.9 (*3.1*)	0.9 (*0.8*)	5.2 (*1.6*)	0.3 (*0.1*)
H99	0.9 (*3.1*)	1.7 (*1.6*)	10 (*3.1*)	10 (*3.1*)
C21F3	0.9 (*3.1*)	0.9 (*0.8*)	5.2 (*1.6*)	<5.2 (<*1.6*)
C. gattii isolates				
WM276	0.9 (*3.1*)	0.9 (*0.8*)	2.6 (*0.8*)	2.6 (*0.8*)
C751	0.9 (*3.1*)	≤0.2 (≤*0.2*)	5.2 (*1.6*)	2.6 (*0.8*)

[a]MIC_{100} or MIC_{50} results by broth microdilution. The inoculum density was 1.25×10^3 cells/ml, and the isolates were incubated for 48 h at 30°C. Each experiment was repeated in duplicate on separate days in at least two different trial experiments. The MIC_{100} or MIC_{50} values are given in micromolar concentrations. The italic values within parentheses are given in micrograms per milliliter.
[b]The average molecular mass of the MM-TM copolymer used for molarity conversion is 3,300 g/mol.
[c]AMB, amphotericin B (molecular mass, 924.091 g/mol).
[d]FLC, fluconazole (molecular mass, 306.271 g/mol).

active against *Aspergillus* spp., displaying MIC_{100} values of >60 μM (>200 μg/ml) in all cases (Table 7). For comparison of MM-TM with drugs currently used to treat aspergillosis, we determined MIC_{100} values for the *Aspergillus* test strains with posaconazole and itraconazole. The results were consistent with previous reports: MIC_{100} values of ~1 μM (~1 μg/ml) for both drugs against azole-sensitive strains and MIC_{100} values of >45 μM (>32 μg/ml) for the azole-resistant strain F11628. Strain F16216 was sensitive to posaconazole (MIC_{100} of 2.5 μM or 1.7 μg/ml) and resistant to itraconazole (MIC_{100} of 45 μM or 32 μg/ml) (Table 7) (25).

Due to the increase in drug-resistant clinical isolates of *A. fumigatus* (26–28) and findings that synergistic effects between azoles and other chemicals have been fruitful in retarding *A. fumigatus* growth (29, 30), we tested MM-TM and the azoles in combination for possible synergistic activity against *Aspergillus*. Using a checkerboard test, we determined the FIC values of these drugs and MM-TM against both azole-sensitive and azole-resistant *A. fumigatus* strains. Overall, we found that MM-TM can exhibit synergistic activity with both posaconazole and itraconazole against both sensitive and resistant strains of *A. fumigatus* (Table 8). Specifically, there was weak synergy (∑FIC index values from 0.1 to 0.3) with both azoles against azole-sensitive strains (AF293 and CEA10), resulting in <7-fold decreases in azole MIC_{100} in the presence of copolymer. In contrast, synergy with both azoles against the azole-resistant strain F11628 was very strong (∑FIC index values of 0.02 and 0.04), resulting in >600-fold and >100-fold decreases in the MIC_{100} values in the presence of MM-TM for posaconazole and

TABLE 6 Synergy checkerboard results with AMB and MM-TM against *Cryptococcus neoformans* H99[a]

Test agent	MIC_{100} of test agent (μM) (μg/ml)[b] Alone[c]	Combination[d]	∑FIC index[e]	FIC interpretation
MM-TM	2.9 (*9.4*)	0.01 (*0.03*)	0.08	Synergistic
AMB	3.4 (*3.1*)	0.16 (*0.15*)		

[a]The inoculum density was 1.25×10^5 cells/ml, and the isolates were incubated for 48 at 30°C. The inoculum density was increased for synergy studies 100-fold to 1.25×10^5 cells/ml relative to MIC studies to ensure there was sufficient inoculum for fungicidal testing. Each experiment was repeated in duplicate on separate days in at least two different trial experiments.
[b]The MIC_{100} values are given in micromolar concentrations. The italic values within parentheses are given in micrograms per milliliter.
[c]MIC as determined by OD_{600} measurements after 48 h for test agent alone.
[d]MIC as determined by OD_{600} measurements after 48 h for test agents incubated with *Cryptococcus* in combination.
[e]Fractional inhibitory concentration (FIC).

TABLE 7 MIC_{100} results for MM-TM against *Aspergillus* spp.[a]

Isolate	MIC_{100} (μM) ($\mu g/ml$)[b]		
	MM-TM[c]	POS[d]	ITRA[e]
A. terreus NIH2624	>61 (*>200*)	1.4 (*1.0*)	1.4 (*1.0*)
A. fumigatus AF293	>61 (*>200*)	2.9 (*2.0*)	1.4 (*1.0*)
A. fumigatus CEA10	>61 (*>200*)	0.7 (*0.5*)	>1.4 (*>1.0*)
A. fumigatus F11628	>61 (*>200*)	>46 (*>32*)	68 (*48*)
A. fumigatus F16216	>61 (*>200*)	2.5 (*1.7*)	45 (*32*)

[a]MIC_{100} results by broth microdilution. The inoculum density was 1×10^5 cells/ml, and the isolates were incubated for 48 h at 35°C. Each experiment was repeated in duplicate on separate days in at least two different trial experiments.
[b]The MIC_{100} values are given in micromolar concentrations. The italic values within parentheses are given in micrograms per milliliter.
[c]The average molecular mass of the MM-TM copolymer used for molarity conversion is 3,300 g/mol.
[d]POS, posaconazole (molecular mass, 700.778 g/mol).
[e]ITRA, itraconazole (molecular mass, 705.64 g/mol).

itraconazole, respectively (Table 8). This finding contrasts with the results for the itraconazole-resistant strain F16216, for which no synergy between the azole and the polymer was detected. This finding was somewhat surprising because the F11628 and F11626 strains have mutations in the same gene, *cyp51A*, which encodes a 14α-sterol demethylase that is involved in ergosterol biosynthesis (Table 2) (29, 31, 32). To probe the relationships between these mutations and synergy, we evaluated MIC_{100} values for MM-TM with either itraconazole or posaconazole against a panel of strains with different combinations of mutations similar to those of strains F11628 and F16216 (see Table S3 in the supplemental material). There was no clear pattern between types of mutations in azole-resistant strains and synergism between an azole and the MM-TM polymer (Tables S4 and S5), which may reflect the considerable heterogeneity among

TABLE 8 Synergy results with azoles and MM-TM against *Aspergillus* spp.[a]

Isolate	Test agent	MIC_{100} of test agent (μM) ($\mu g/ml$)[b]		∑FIC index[e]	FIC interpretation
		Alone[c]	Combination[d]		
A. fumigatus AF293	MM-TM	>30 (*>100*)[e]	1.2 (*3.9*)	0.23	Synergistic
	Posaconazole	1.6 (*1.1*)	0.3 (*0.2*)		
	MM-TM	>30 (*>100*)[e]	1.2 (*3.9*)	0.22	Synergistic
	Itraconazole	1.7 (*1.2*)	0.3 (*0.2*)		
A. fumigatus CEA10	MM-TM	>30 (*>100*)[e]	0.5 (*1.6*)	0.20	Synergistic
	Posaconazole	0.7 (*0.5*)	0.1 (*0.1*)		
	MM-TM	>30 (*>100*)[e]	0.5 (*1.6*)	0.11	Synergistic
	Itraconazole	>1.4 (*>1.0*)	0.3 (*0.2*)		
A. fumigatus F11628	MM-TM	>30 (*>100*)[e]	1.2 (*3.9*)	0.02	Synergistic
	Posaconazole	100 (*72*)	0.1 (*0.1*)		
	MM-TM	>30 (*>100*)[e]	2.1 (*7.0*)	0.04	Synergistic
	Itraconazole	100 (*72*)	0.6 (*0.4*)		
A. fumigatus F16216	MM-TM	>30 (*>100*)[e]	0.5 (*1.6*)	0.57	Indifferent
	Posaconazole	2.5 (*1.8*)	1.4 (*1.0*)		
	MM-TM	>30 (*>100*)[e]	>30 (*>100*)[e]	1.44	Indifferent
	Itraconazole	91 (*64*)	85 (*60*)		

[a]Synergy results with azoles and MM-TM (40:60). The inoculum density was 1×10^5 cells/ml, and the isolates were incubated for 48 h at 35°C. Each experiment was repeated in duplicate on separate days in at least two different trial experiments.
[b]The MIC_{100} values are given in micromolar concentrations. The italic values within parentheses are given in micrograms per milliliter.
[c]MIC after 48 h for the test agent alone.
[d]FIC, fractional inhibitory concentration.
[e]The high off-scale MIC value, >30.3 μM, was converted to the next highest concentration, 60.6 μM, for calculation of the FIC index.

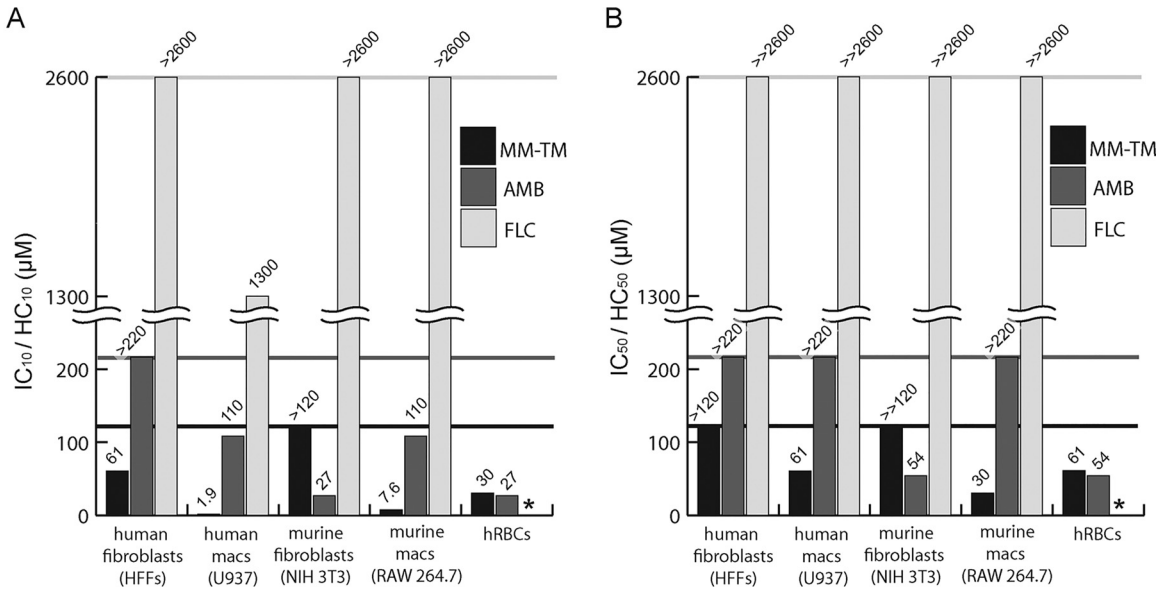

FIG 3 Lytic effects of MM-TM and conventional antifungal agents on mammalian cells. Human foreskin fibroblasts (HFFs), human differentiated macrophages (U937), murine fibroblasts (NIH 3T3), murine macrophages (macs) (RAW 264.7), and human red blood cells (hRBCs) were tested in dilution series of concentrations of MM-TM, amphotericin B (AMB), and fluconazole (FLC). The percentage of cell lysis for each compound was compared to no treatment (0% lysis) and complete lysis (detergent) controls. Solid horizontal lines represent the highest concentrations tested in each dilution series (120 μM for MM-TM, 220 μM for AMB, and 2,600 μM for FLC). Note that higher bars indicate lower lytic potency. (A) The concentration of drug necessary to cause lysis of 10% of macrophages/fibroblasts (IC_{10}) or lysis of 10% of hRBCs ("hemolysis"; HC_{10}). (B) The concentration of drug necessary to cause lysis of 50% of macrophages/fibroblasts (IC_{50}) or 50% of hRBCs (HC_{50}). In cases where IC_{50} or HC_{50} values were between two concentrations in the dilution series, the lower concentration is reported. hRBCs that were not tested with FLC are indicated by an asterisk.

A. fumigatus strains (29, 33). These results indicate that whether synergy is observed for MM-TM/azole combinations is dependent on unknown properties of the strains.

MM-TM shows variable toxicity toward mammalian cells. To determine the cytotoxicity profile of the MM-TM copolymer on mammalian cells, we evaluated the ability of MM-TM to induce lysis of fibroblasts, macrophages, and red blood cells as a function of polymer concentration. Comparable studies were conducted with AMB and FLC. These experiments employed human foreskin fibroblasts (HFFs), human differentiated mouse macrophages (U937), mouse fibroblasts (NIH 3T3), mouse macrophages (RAW 264.7), and human red blood cells (hRBCs). Fibroblasts and macrophages were incubated for 12 h in the presence of a dilution series of copolymer, AMB, or FLC. hRBCs were incubated for 1 h with a dilution series of copolymer or AMB. The percentage of cells lysed by each treatment was measured by release of lactate dehydrogenase (LDH) (fibroblasts and macrophages) or hemoglobin (hRBCs) and compared to control measurements for 0% lysis (no treatment) and for 100% lysis (Triton X-100) to determine the amount of each agent that would cause 10% or 50% lysis (10% inhibitory concentration [IC_{10}] or IC_{50} for macrophages or fibroblasts; 10% hemolysis concentration [HC_{10}] or HC_{50} for hRBCs).

MM-TM exhibited a lower propensity to lyse fibroblasts compared to macrophages (Fig. 3, black bars, and Fig. S7). Fifteen times more MM-TM was required to lyse 10% of fibroblasts (HFFs and NIH 3T3) relative to the concentration required to lyse 10% of macrophages (U937 and RAW 264.7) (Fig. 3A). A similar trend was observed for the concentrations required to lyse 50% of cells (Fig. 3B). In assays with human red blood cells, 10% and 50% hemolysis were observed at 30 and 61 μM (100 and 200 μg/ml), respectively. These levels of hemolysis were comparable to those observed with AMB (Fig. 3 and Fig. S10 and S11).

Like MM-TM, AMB showed a very low propensity to lyse human fibroblasts (HFFs), with less than 10% lysis observed at the highest concentration tested (220 μM or 200 μg/ml) (Fig. 3 and Fig. S8). However, AMB was significantly more lytic toward murine

fibroblasts (NIH 3T3), lysing 10% and 50% of NIH 3T3 cells at 27 μM and 54 μM (25 and 50 μg/ml), respectively. For both human and murine macrophages, AMB caused lysis at similar concentrations (110 μM or 100 μg/ml for 10% lysis and >220 μM or >200 μg/ml for 50% lysis). As anticipated, FLC showed negligible lytic effects toward all cells tested (Fig. S9). From these data, we conclude that MM-TM is more lytic toward mammalian cells than fluconazole is; however, both MM-TM and AMB display a variable lytic profile toward mammalian cells. While MM-TM shows apparent higher lytic activity than AMB does in some cases, the concentration of MM-TM needed to inhibit fungi as a solo agent or in combination with AMB or an azole is often much lower than the concentrations required for mammalian cell lysis. For example, *C. neoformans* (H99) is 100% inhibited by MM-TM at 0.9 μM (3.1 μg/ml), a concentration that would be expected to have almost no lytic effect on fibroblasts and to lyse <5% of human macrophages (Fig. S7). In synergy studies, only 0.5 μM (1.6 μg/ml) MM-TM was needed to inhibit *A. fumigatus* (CEA10) growth in the presence of posaconazole (0.1 μM or 0.1 μg/ml). Given the ability of MM-TM to exhibit favorable antifungal activities at low concentrations, this polymer is a promising candidate for further investigation.

In a separate toxicity study not based on cell lysis, MM-TM was tested against *Arabidopsis thaliana* seedlings to assess its effects on plant growth. Fungicide resistance in fungal phytopathogens is a growing concern (34, 35), and *A. thaliana* is often used to assess off-target effects of potential fungicides (36, 37). At 0.3 μM and 3.0 μM (1 and 10 μg/ml) MM-TM, seedlings appeared to grow normally, and root growth was not statistically different from that of the controls. At 30 μM (100 μg/ml) MM-TM, however, root growth decreased by roughly 40%, and the roots themselves displayed an unusual waving and rightward skewing behavior (Fig. S12). These results indicate that at high concentrations, the MM-TM copolymer has negative effects on *A. thaliana*, but at lower concentrations (to which fungi are susceptible), MM-TM does not adversely affect germination or growth of *A. thaliana*.

DISCUSSION

The high cost of synthesizing sequence-specific peptides on a large scale constitutes a significant barrier to the development of HDPs or related sequence-specific oligomers for therapeutic use (2, 7). This limitation has led many research groups to study the antimicrobial properties of synthetic, amphipathic polymers (11, 12, 16, 38–52), an approach inspired by the observation that HDPs with diverse amino acid compositions and sizes display similar growth-inhibitory activities against bacteria (53). Nylon-3 copolymers were among the first reported materials to manifest an HDP-like activity profile, inhibiting the growth of diverse bacteria but displaying very low hemolytic activity (11).

Recent work has broadened the range of nylon-3 polymer functions by demonstration of antifungal activity (13, 14). Here we augment this development by describing a new nylon-3 copolymer, MM-TM, that shows excellent activity against a diverse set of invasive human fungal pathogens and relatively low toxicity toward mammalian cells. The fungi used in this study were chosen on the basis of their clinical relevance, phylogenetic diversity, and the wealth of genetic, molecular, bioinformatic, and animal tools available to study each genus. Collectively, these pathogens account for >75% of fungus-caused fatalities (15). Two are ascomycetes (*Candida* and *Aspergillus*), each with diverse properties (yeast versus filamentous fungus), and the third is a basidiomycete yeast (*Cryptococcus*). These three fungal genera have been the subjects of intense study and therefore represent model systems in the field of mycology (18).

The MM-TM copolymer displays good activity against *Candida* spp. and excellent activity against *Cryptococcus* spp. as a stand-alone agent. The MM-TM polymer displays strong synergistic activity with azole drugs against *C. albicans* and *A. fumigatus*, even against some azole-resistant strains. The latter finding is especially promising, as many studies are turning to combination approaches to stem the rise of resistance to conventional antifungal drugs and preserve activity of the limited number of therapeutic antifungal drugs available thus far (29, 30). The decreased MIC_{100} values ($\leq$1 μM

and ≤3 μg/ml) of MM-TM against select strains of *Candida*, *Cryptococcus*, and *Aspergillus* in combination with either azoles or AMB highlight the potential of MM-TM in the combination format. Combination therapy represents a promising strategy to enhance the efficacy of antifungals and improve clinical outcomes by decreasing the emergence of drug resistance, reducing dosages, and avoiding host toxicity associated with an already limited panel of available antifungal drugs.

Many current antifungal drugs, particularly AMB, are relatively toxic to the human host (19). We found that the lytic effects of MM-TM on selected mammalian cell types were on par with or greater than those of AMB, but cell type-specific variations in lytic activity were observed. The relatively low lytic activity of MM-TM toward fibroblasts and hRBCs is promising in terms of future development. In contrast, the relatively high lytic activity of the nylon-3 copolymer toward macrophages could be problematic in this regard. However, this difference in lytic effects among cell types could provide interesting opportunities in antifungal compound development. For example, elucidating the mechanism of differential lytic propensities toward mammalian cells could provide insights regarding the MM-TM mechanism of action against fungi. Phagocyte-specific lytic activity could be exploited against fungal pathogens (such as *Cryptococcus*) that have been proposed to use phagocytes as Trojan horses in which to disseminate in the host or to lie dormant for long periods of time (20). Targeting pathogen-harboring phagocytes could be a strategy for limiting fungal dissemination. In this regard, we note that the polymer concentration leading to 10% macrophage lysis (7.6 μM or 25 μg/ml) is somewhat higher than the MIC_{100} for the *Cryptococcus* species we evaluated (0.9 μM or 3.1 μg/ml). Thus, it might be possible to eliminate an invading pathogen while sparing most host cells. Even if it is not possible to exploit the lytic activity of MM-TM toward macrophages, the comparably low lytic activity toward dermal fibroblasts (HFFs) indicates that the polymer could be well suited for development as a topical antifungal agent.

The remarkable activity of the MM-TM copolymer, a nontraditional chemotype for drug development, against diverse fungi suggests that optimization could lead to an effective broad-spectrum antifungal agent. The chemistry of nylon-3 polymers facilitates modification of polymer structure and composition in pursuit of broad-spectrum agents or customized materials with activity against a particular fungus (11–14, 54). Furthermore, the chemistry allows for optimization of antifungal agents for either combination therapy with current drugs or for mass production as a topical agent.

Conclusion. Our demonstration of antifungal activity against pathogenic species in multiple genera by a new nylon-3 copolymer, MM-TM, offers the prospect of a nontraditional strategy for developing agents to treat fungal disease. Examination of this sequence-random copolymer was inspired by the antifungal activities reported for naturally occurring sequence-specific peptides; the copolymer, however, is much easier to synthesize than a sequence-specific peptide is. Although the polymer exerts moderate lytic effects on some mammalian cells, it might be possible to minimize this source of toxicity via synergistic combinations of the polymer with an established antifungal drug, both at low concentrations. In certain cases, it might be possible to harness selective polymer lytic activity toward macrophages for anticryptococcal therapy. The results described here provide a motivation for determining the mechanism(s) by which MM-TM and other nylon-3 polymers kill fungi.

MATERIALS AND METHODS

Fungal strain maintenance. All strains were handled using standard techniques and media as described previously (55). *Candida* and *Cryptococcus* strains were grown on yeast extract-peptone-dextrose (YPD) agar plates and stored at 4°C. *Candida* and *Cryptococcus* strains were cultured overnight in liquid media at 30°C and washed with phosphate-buffered saline (PBS) prior to MIC_{100} (MIC that inhibits 100% growth), minimum fungicidal concentration (MFC), and synergy studies. *Aspergillus* strains were maintained as glycerol stocks at −80°C and propagated on glucose-containing minimal medium (GMM) at 37°C (56). Spores were harvested in 0.01% Tween 80, enumerated using a hemacytometer, and used for MIC_{100}, MFC, and synergy studies immediately postharvest.

Synthesis, purification, and characterization of the MM-TM random copolymers. Nylon-3 copolymers were synthesized and purified as described previously (11, 12); in the β-lactam MMβ, the side

chain amino group is protected by *tert*-butyloxycarbonyl (Boc). For dispersity and molecular mass determinations, the copolymer with Boc side chain protecting groups intact was analyzed by gel permeation chromatography (GPC) using *N*,*N*-dimethylacetamide (DMAc) as the mobile phase. The degree of polymerization determined by GPC (Dp_{GPC}) or average number of subunits per chain was calculated based on the number-average molecular mass (M_n) value from GPC data, the nuclear magnetic resonance (NMR)-determined average ratio of subunits per polymer chain, and the molecular masses of the subunits using the equation below

$$\mathrm{Dp_{GPC}} = \left(M_n - M_{\mathrm{eg}}\right)/\left[M_{\mathrm{MM}}x = M_{\mathrm{TM}}\left(1 - x\right)\right]$$

where M_{eg} is the mass of the N-terminal end group (*t*-BuC_6H_4-CO- [*t*-Bu is *tert*-butyl]), M_{MM} is the mass of the MM subunit with the side chain protecting group intact, M_{TM} is the mass of the TM subunit, and *x* is the mole fraction of MM subunit as determined via NMR. Nylon-3 copolymers after deprotection of the side chain amino groups were characterized by ^{1}H NMR. The degree of polymerization determined by NMR (Dp_{NMR}) or average number of subunits per chain was calculated from NMR integrations of resonances characteristic of one of the subunits (see Tables S1 and S2 in the supplemental material). Please see the supplemental material for a more detailed explanation of the synthesis, purification, and characterization of the MM-TM random copolymers.

Antifungal activity assays. MIC_{100} values for *Candida* and *Cryptococcus* spp. were determined by the broth microdilution method according to the CLSI M27-A3 guidelines (17), with slight modifications. In brief, fungal cells at a density of 1.25×10^3 cells/ml were incubated in RPMI 1640 plus 0.145 M 3-(*N*-morpholino)propanesulfonic acid (MOPS), pH 7.0, in 96-well plates with twofold serial dilutions of MM-TM copolymer (0.06 to 60.6 μM or 0.2 to 200 μg/ml), amphotericin B (AMB) (0.22 to 216 μM or 0.2 to 200 μg/ml), or fluconazole (FLC) (0.3 to 653 μM or 0.1 to 200 μg/ml). After 24 h or 48 h for *Candida* and *Cryptococcus* spp., respectively, the optical density at 600 nm (OD_{600}) of each well was measured using a microplate reader. Wells containing fungal cells with no drug and wells containing only RPMI 1640 were used as positive and blank controls, respectively. Percent cell growth was determined as follows: [(sample absorbance − blank absorbance)/(control absorbance − blank absorbance)] × 100%. The MIC_{100} endpoint of each antifungal agent was determined as the lowest concentration to inhibit 100% of fungal growth compared to the no-drug control. All values reported represent the average MIC_{100} concentration of two or more biological replicates and two or more technical replicates each. The average MIC_{100} value consistently fell within a twofold serial dilution of the concentration of each experimental replicate.

The MIC_{100} values for *Aspergillus* spp. were determined by the broth microdilution method according to the European Committee for Antimicrobial Susceptibility Testing (EUCAST) Subcommittee on Antifungal Susceptibility Testing (AFST) *Aspergillus* guidelines (57, 58). Briefly, *Aspergillus* conidia at a density of 1×10^5 conidia/ml were incubated in 96-well plates with twofold serial dilutions of the MM-TM copolymer (0.9 to 60.6 μM or 3.1 to 100 μg/ml), posaconzole (1.1 to 68.5 μM or 0.75 to 48 μg/ml), or itraconazole (0.7 to 45.3 μM or 0.5 to 32 μg/ml) in RPMI 1640 plus 0.145 M MOPS supplemented with 2% glucose. After 48 h at 35°C, the MIC_{100} endpoint of each antifungal agent was determined as the lowest concentration to inhibit 100% of hyphal outgrowth from conidia. All values reported represent the average MIC_{100} value of two or more biological replicates and two or more technical replicates each. The average MIC_{100} value consistently fell within a twofold serial dilution of the concentration of each experimental replicate.

Synergy studies. Synergistic drug interactions were evaluated using a checkerboard microdilution approach interpreted using the method of lowest FIC index (59). For *C. albicans* and *C. neoformans*, fungal cells at a density of 1.25×10^5 cells/ml were incubated in 96-well plates with twofold serial dilutions of either FLC (0 to 81.6 μM or 0 to 25 μg/ml) or AMB (0 to 6.8 μM or 0 to 6.3 μg/ml) and the nylon-3 copolymer MM-TM (0 to 15.2 μM or 0 to 50 μg/ml) in RPMI 1640 plus 0.145 M MOPS, pH 7.0. After 48 h, the OD_{600} of each well was measured using a microplate reader. The MIC_{100} endpoint of the drugs alone or in combination was determined as the lowest concentration to inhibit 100% of fungal growth compared to the no-drug control.

A. fumigatus synergistic drug interactions were also evaluated using a checkerboard microdilution method. *A. fumigatus* conidia at a density of 1×10^5 conidia/ml were incubated in 96-well plates with 0.25-fold or 2-fold serial dilutions of either posaconazole (0 to 68.5 μM or 0 to 48 μg/ml) or itraconazole (0 to 68.0 μM or 0 to 48 μg/ml) and nylon-3 copolymer MM-TM (0 to 30.3 μM or 0 to 100 μg/ml) in RPMI 1640 plus 0.145 M MOPS (pH 7.0) supplemented with 2% glucose. Posaconazole or itraconazole plus copolymer concentrations were tailored to the antifungal agent and *A. fumigatus* strains used in each assay. The MIC_{100}s of the drugs alone and in combination were determined as the lowest drug concentrations preventing hyphal outgrowth from conidia.

The sum of the fractional inhibitory concentrations ($\sum$FIC) was calculated as follows for assessing synergy: $\sum FIC = \sum FIC_A + \sum FIC_B$, where $\sum FIC_A$ = (MIC_{100} of antifungal A in combination/MIC_{100} of antifungal A alone) where the "MIC_{100} of antifungal A alone" is the MIC_{100} of antifungal A when used as a sole agent. The "MIC_{100} of antifungal A in combination" is the MIC_{100} of antifungal A when used in combination with agent B. When the MIC_{100} of the antifungal agent alone or in combination did not fall within the range of concentrations tested, the next serial dilution higher was used as the MIC_{100}. The following values were used as cutoffs: ≤0.5 for synergism; >0.5 and ≤4 for indifference; and >4 for antagonism.

Hemolysis. Hemolysis assays were performed using expired human red blood cells (hRBCs) obtained from the University of Wisconsin–Madison hospital as described previously (60). Twofold serial dilutions of MM-TM (0.9 to 121.2 μM or 3.1 to 400 μg/ml) and AMB (3.4 to 432.8 μM or 3.1 to 400 μg/ml) dissolved

in Tris-buffered saline (TBS) (10 mM Tris, 150 mM NaCl [pH 7.2]) were incubated with 2% (vol/vol) hRBC suspension in TBS. hRBCs treated with TBS only and hRBCs treated with a 20% Triton X-100 solution in TBS were used as the blank and positive control, respectively. Assays were performed in 96-well plates, with a total volume of 200 μl per well, and incubated for 1 h at 37°C. After incubation and centrifugation, the OD_{405} values of the supernatants were measured. The percent hemolysis for each sample was calculated as [(sample absorbance − blank absorbance)/(control absorbance − blank absorbance)] × 100%.

Lysis of fibroblasts and macrophages. The lytic activities of MM-TM toward differentiated U937 macrophages, human foreskin fibroblasts (HFFs), NIH 3T3 fibroblasts, and RAW 264.7 macrophages were evaluated side by side with the lytic activities of AMB and FLC using the CytoTox-ONE assay kit (Promega). U937 cells were cultured as nonadherent cells in RPMI 1640 plus 10% fetal bovine serum (FBS), 1 mM sodium pyruvate, and 2 mM L-glutamine and differentiated into macrophages in 96-well plates (5×10^5 cells/well) by 14-h incubation with 50 ng/ml phorbol 12-myristate 13-acetate (PMA) followed by 60 h without PMA. Confluent HFFs in Dulbecco modified Eagle medium (DMEM) plus 10% 2 mM L-glutamine, 1.5×10^4 NIH 3T3 cells/well in DMEM plus 10% FBS, or 1×10^4 RAW 264.7 cells/well in RPMI plus 10% FBS and 2 mM glutamine were passaged into 96-well plates and grown at 37°C and 5% CO_2 (up to 2 weeks for HFFs and 24 h for NIH 3T3 and RAW 264.7 cells). For all cultured mammalian cells, medium was removed, and twofold serial dilution series of MM-TM (0.9 to 121.2 μM or 3.1 to 400 μg/ml), AMB (1.7 to 216 μM or 1.6 to 200 μg/ml), or FLC (20.4 to 2,612 μM or 6.3 to 800 μg/ml) were added to the wells in triplicate with a total volume of 100 μl of cell culture medium per well. The plates were incubated at 37°C and 5% CO_2 for 12 h. Cells in culture medium only served as the negative lysis control (blank), and cells treated with a lysate solution of Triton X-100 to cause 100% lysis (full toxicity) served as a positive control. Fluorescence intensity was measured on a Tecan Infinite M1000 microplate reader using excitation/emission wavelengths of 560/590 nm. Cytotoxicity was calculated as follows: % cell death = $(F^{\text{treatment}} - F^{\text{blank}})/(F^{\text{lysed}} - F^{\text{blank}}) \times 100\%$ where $F^{\text{treatment}}$ is the fluorescent intensity of the treated cells. IC_{10} and IC_{50} were determined as the concentration of drug that caused 10% or 50% cell lysis, respectively (or the lower of the two dilutions that fall on either side of 10% or 50% cell death).

SUPPLEMENTAL MATERIAL

Supplemental material for this article may be found at https://doi.org/10.1128/AAC.00204-17.

SUPPLEMENTAL FILE 1, PDF file, 0.9 MB.

ACKNOWLEDGMENTS

This study was supported in part by UW SDRC grant P30 AR066524 (S.H.G., N.P.K., and C.M.H.), USDA Hatch Formula Fund WIS01710 (N.P.K.), NIH grant R01 AI065728 (N.P.K.), NIH grant R01 GM093265 (S.H.G.), NIH T32 GM007215 (N.M.W.), and NIH R01 AI089370 (C.M.H.).

We thank Sarah Wilson, Nate Teachout, and Laura Knoll for supplying and culturing the HFFs and Erin Theisen and J. D. Sauer for supplying U937 cells. We thank Amy Jancewicz and Patrick Masson for assistance performing toxicity assays on *Arabidopsis thaliana* seedlings.

REFERENCES

1. Zasloff M. 2002. Antimicrobial peptides of multicellular organisms. Nature 415:389–395. https://doi.org/10.1038/415389a.
2. Hancock REW, Sahl H-G. 2006. Antimicrobial and host-defense peptides as new anti-infective therapeutic strategies. Nat Biotechnol 24:1551–1557. https://doi.org/10.1038/nbt1267.
3. van der Weerden NL, Bleackley MR, Anderson MA. 2013. Properties and mechanisms of action of naturally occurring antifungal peptides. Cell Mol Life Sci 70:3545–3570. https://doi.org/10.1007/s00018-013-1260-1.
4. Yeaman MR, Yount NY. 2003. Mechanisms of antimicrobial peptide action and resistance. Pharmacol Rev 55:27–55. https://doi.org/10.1124/pr.55.1.2.
5. Wilmes M, Cammue BPA, Sahl H-G, Thevissen K. 2011. Antibiotic activities of host defense peptides: more to it than lipid bilayer perturbation. Nat Prod Rep 28:1350–1358. https://doi.org/10.1039/c1np00022e.
6. Silva PM, Gonçalves S, Santos NC. 2014. Defensins: antifungal lessons from eukaryotes. Front Microbiol 5:97. https://doi.org/10.3389/fmicb.2014.00097.
7. Marr AK, Gooderham WJ, Hancock RE. 2006. Antibacterial peptides for therapeutic use: obstacles and realistic outlook. Curr Opin Pharmacol 6:468–472. https://doi.org/10.1016/j.coph.2006.04.006.
8. Ilker MF, Nüsslein K, Tew GN, Coughlin EB. 2004. Tuning the hemolytic and antibacterial activities of amphiphilic polynorbornene derivatives. J Am Chem Soc 126:15870–15875. https://doi.org/10.1021/ja045664d.
9. Gelman MA, Weisblum B, Lynn DM, Gellman SH. 2004. Biocidal activity of polystyrenes that are cationic by virtue of protonation. Org Lett 6:557–560. https://doi.org/10.1021/ol036341+.
10. Kuroda K, DeGrado WF. 2005. Amphiphilic polymethacrylate derivatives as antimicrobial agents. J Am Chem Soc 127:4128–4129. https://doi.org/10.1021/ja044205+.
11. Mowery BP, Lee SE, Kissounko DA, Epand RF, Epand RM, Weisblum B, Stahl SS, Gellman SH. 2007. Mimicry of antimicrobial host-defense peptides by random copolymers. J Am Chem Soc 129:15474–15476. https://doi.org/10.1021/ja077288d.
12. Mowery BP, Lindner AH, Weisblum B, Stahl SS, Gellman SH. 2009. Structure-activity relationships among random nylon-3 copolymers that mimic antibacterial host-defense peptides. J Am Chem Soc 131:9735–9745. https://doi.org/10.1021/ja901613g.
13. Liu R, Chen X, Hayouka Z, Chakraborty S, Falk SP, Weisblum B, Masters KS, Gellman SH. 2013. Nylon-3 polymers with selective antifungal activity. J Am Chem Soc 135:5270–5273. https://doi.org/10.1021/ja4006404.
14. Liu R, Chen X, Falk SP, Mowery BP, Karlsson AJ, Weisblum B, Palecek SP, Masters KS, Gellman SH. 2014. Structure–activity relationships among antifungal nylon-3 polymers: identification of materials active against

drug-resistant strains of *Candida albicans*. J Am Chem Soc 136:4333–4342. https://doi.org/10.1021/ja500036r.
15. Brown GD, Denning DW, Gow NAR, Levitz SM, Netea MG, White TC. 2012. Hidden killers: human fungal infections. Sci Transl Med 4:165rv13. https://doi.org/10.1126/scitranslmed.3004404.
16. Abd-El-Aziz AS, Agatemor C, Etkin N, Overy DP, Lanteigne M, McQuillan K, Kerr RG. 2015. Antimicrobial organometallic dendrimers with tunable activity against multidrug-resistant bacteria. Biomacromolecules 16:3694–3703. https://doi.org/10.1021/acs.biomac.5b01207.
17. Clinical and Laboratory Standards Institute. 2008. Approved standard M27-A3. Reference method for broth dilution antifungal susceptibility testing of yeasts, 3rd ed. Clinical and Laboratory Standards Institute, Wayne, PA.
18. Karkowska-Kuleta J, Rapala-Kozik M, Kozik A. 2009. Fungi pathogenic to humans: molecular bases of virulence of *Candida albicans*, *Cryptococcus neoformans* and *Aspergillus fumigatus*. Acta Biochim Pol 56:211–224.
19. Roemer T, Krysan DJ. 2014. Antifungal drug development: challenges, unmet clinical needs, and new approaches. Cold Spring Harb Perspect Med 4:a019703. https://doi.org/10.1101/cshperspect.a019703.
20. Taylor-Smith LM, May RC. 2016. New weapons in the *Cryptococcus infection* toolkit. Curr Opin Microbiol 34:67–74. https://doi.org/10.1016/j.mib.2016.07.018.
21. Pierce AM, Pierce HD, Jr, Unrau AM, Oehlschlager AC. 1978. Lipid composition and polyene antibiotic resistance of *Candida albicans* mutants. Can J Biochem 56:135–142. https://doi.org/10.1139/o78-023.
22. Vazquez JA. 2007. Role of posaconazole in the management of oropharyngeal and esophageal candidiasis. Ther Clin Risk Manag 3:533–542.
23. Franz R, Ruhnke M, Morschhäuser J. 1999. Molecular aspects of fluconazole resistance development in *Candida albicans*. Mycoses 42:453–458. https://doi.org/10.1046/j.1439-0507.1999.00498.x.
24. Shrestha SK, Grilley M, Anderson T, Dhiman C, Oblad J, Chang C-WT, Sorensen KN, Takemoto JY. 2015. In vitro antifungal synergy between amphiphilic aminoglycoside K20 and azoles against *Candida* species and *Cryptococcus neoformans*. Med Mycol 53:837–844. https://doi.org/10.1093/mmy/myv063.
25. Arendrup MC, Jensen RH, Cuenca-Estrella M. 2015. In vitro activity of ASP2397 against *Aspergillus* isolates with or without acquired azole resistance mechanisms. Antimicrob Agents Chemother 60:532–536. https://doi.org/10.1128/AAC.02336-15.
26. Howard SJ, Cerar D, Anderson MJ, Albarrag A, Fisher MC, Pasqualotto AC, Laverdiere M, Arendrup MC, Perlin DS, Denning DW. 2009. Frequency and evolution of azole resistance in *Aspergillus fumigatus* associated with treatment failure. Emerg Infect Dis 15:1068–1076. https://doi.org/10.3201/eid1507.090043.
27. Denning DW, Park S, Lass-Florl C, Fraczek MG, Kirwan M, Gore R, Smith J, Bueid A, Moore CB, Bowyer P, Perlin DS. 2011. High-frequency triazole resistance found in nonculturable *Aspergillus fumigatus* from lungs of patients with chronic fungal disease. Clin Infect Dis 52:1123–1129. https://doi.org/10.1093/cid/cir179.
28. Verweij PE, Ananda-Rajah M, Andes D, Arendrup MC, Brüggemann RJ, Chowdhary A, Cornely OA, Denning DW, Groll AH, Izumikawa K, Kullberg BJ, Lagrou K, Maertens J, Meis JF, Newton P, Page I, Seyedmousavi S, Sheppard DC, Viscoli C, Warris A, Donnelly JP. 2015. International expert opinion on the management of infection caused by azole-resistant *Aspergillus fumigatus*. Drug Resist Updat 21–22:30–40.
29. Mavridou E, Meletiadis J, Rijs A, Mouton JW, Verweij PE. 2015. The strength of synergistic interaction between posaconazole and caspofungin depends on the underlying azole resistance mechanism of *Aspergillus fumigatus*. Antimicrob Agents Chemother 59:1738–1744. https://doi.org/10.1128/AAC.04469-14.
30. Li S-X, Song Y-J, Jiang L, Zhao Y-J, Guo H, Li D-M, Zhu K-J, Zhang H. 12 January 2017. Synergistic effects of tetrandrine with posaconazole against *Aspergillus fumigatus*. Microb Drug Resist https://doi.org/10.1089/mdr.2016.0217.
31. Afeltra J, Vitale RG, Mouton JW, Verweij PE. 2004. Potent synergistic in vitro interaction between nonantimicrobial membrane-active compounds and itraconazole against clinical isolates of *Aspergillus fumigatus* resistant to itraconazole. Antimicrob Agents Chemother 48:1335–1343. https://doi.org/10.1128/AAC.48.4.1335-1343.2004.
32. Mellado E, Garcia-Effron G, Alcázar-Fuoli L, Melchers WJG, Verweij PE, Cuenca-Estrella M, Rodríguez-Tudela JL. 2007. A new *Aspergillus fumigatus* resistance mechanism conferring in vitro cross-resistance to azole antifungals involves a combination of cyp51A alterations. Antimicrob Agents Chemother 51:1897–1904. https://doi.org/10.1128/AAC.01092-06.
33. Keller NP. 2017. Heterogeneity confounds establishment of "a" model microbial strain. mBio 8:e00135-17. https://doi.org/10.1128/mBio.00135-17.
34. Hahn M. 2014. The rising threat of fungicide resistance in plant pathogenic fungi: *Botrytis* as a case study. J Chem Biol 7:133–141. https://doi.org/10.1007/s12154-014-0113-1.
35. Mohd-Assaad N, McDonald BA, Croll D. 2016. Multilocus resistance evolution to azole fungicides in fungal plant pathogen populations. Mol Ecol 25:6124–6142. https://doi.org/10.1111/mec.13916.
36. Oh K, Matsumoto T, Yamagami A, Hoshi T, Nakano T, Yoshizawa Y. 2015. Fenarimol, a pyrimidine-type fungicide, inhibits brassinosteroid biosynthesis. Int J Mol Sci 16:17273–17288. https://doi.org/10.3390/ijms160817273.
37. Atanasov KE, Barboza-Barquero L, Tiburcio AF, Alcázar R. 2016. Genome wide association mapping for the tolerance to the polyamine oxidase inhibitor guazatine in *Arabidopsis thaliana*. Front Plant Sci 7:401. https://doi.org/10.3389/fpls.2016.00401.
38. Sellenet PH, Allison B, Applegate BM, Youngblood JP. 2007. Synergistic activity of hydrophilic modification in antibiotic polymers. Biomacromolecules 8:19–23. https://doi.org/10.1021/bm0605513.
39. Lienkamp K, Madkour AE, Musante A, Nelson CF, Nüsslein K, Tew GN. 2008. Antimicrobial polymers prepared by ROMP with unprecedented selectivity: a molecular construction kit approach. J Am Chem Soc 130:9836–9843. https://doi.org/10.1021/ja801662y.
40. Sambhy V, Peterson BR, Sen A. 2008. Antibacterial and hemolytic activities of pyridinium polymers as a function of the spatial relationship between the positive charge and the pendant alkyl tail. Angew Chem Int Ed Engl 47:1250–1254. https://doi.org/10.1002/anie.200702287.
41. Palermo EF, Sovadinova I, Kuroda K. 2009. Structural determinants of antimicrobial activity and biocompatibility in membrane-disrupting methacrylamide random copolymers. Biomacromolecules 10:3098–3107. https://doi.org/10.1021/bm900784x.
42. Song A, Walker SG, Parker KA, Sampson NS. 2011. Antibacterial studies of cationic polymers with alternating, random, and uniform backbones. ACS Chem Biol 6:590–599. https://doi.org/10.1021/cb100413w.
43. Nederberg F, Zhang Y, Tan JPK, Xu K, Wang H, Yang C, Gao S, Guo XD, Fukushima K, Li L, Hedrick JL, Yang Y-Y. 2011. Biodegradable nanostructures with selective lysis of microbial membranes. Nat Chem 3:409–414. https://doi.org/10.1038/nchem.1012.
44. Li P, Zhou C, Rayatpisheh S, Ye K, Poon YF, Hammond PT, Duan H, Chan-Park MB. 2012. Cationic peptidopolysaccharides show excellent broad-spectrum antimicrobial activities and high selectivity. Adv Mater 24:4130–4137. https://doi.org/10.1002/adma.201104186.
45. Jiang Y, Yang X, Zhu R, Hu K, Lan W-W, Wu F, Yang L. 2013. Acid-activated antimicrobial random copolymers: a mechanism-guided design of antimicrobial peptide mimics. Macromolecules 46:3959–3964. https://doi.org/10.1021/ma400484b.
46. Locock KES, Michl TD, Valentin JDP, Vasilev K, Hayball JD, Qu Y, Traven A, Griesser HJ, Meagher L, Haeussler M. 2013. Guanylated polymethacrylates: a class of potent antimicrobial polymers with low hemolytic activity. Biomacromolecules 14:4021–4031. https://doi.org/10.1021/bm401128r.
47. Costanza F, Padhee S, Wu H, Wang Y, Revenis J, Cao C, Li Q, Cai J. 2013. Investigation of antimicrobial PEG-poly(amino acid)s. RSC Adv 4:2089–2095. https://doi.org/10.1039/C3RA44324H.
48. Chin W, Yang C, Ng VWL, Huang Y, Cheng J, Tong YW, Coady DJ, Fan W, Hedrick JL, Yang YY. 2013. Biodegradable broad-spectrum antimicrobial polycarbonates: investigating the role of chemical structure on activity and selectivity. Macromolecules 46:8797–8807. https://doi.org/10.1021/ma4019685.
49. Krumm C, Harmuth S, Hijazi M, Neugebauer B, Kampmann A-L, Geltenpoth H, Sickmann A, Tiller JC. 2014. Antimicrobial poly(2-methyloxazoline)s with bioswitchable activity through satellite group modification. Angew Chem Int Ed Engl 53:3830–3834. https://doi.org/10.1002/anie.201311150.
50. Michl TD, Locock KES, Stevens NE, Hayball JD, Vasilev K, Postma A, Qu Y, Traven A, Haeussler M, Meagher L, Griesser HJ. 2014. RAFT-derived antimicrobial polymethacrylates: elucidating the impact of end-groups on activity and cytotoxicity. Polym Chem 5:5813–5822. https://doi.org/10.1039/C4PY00652F.
51. Strassburg A, Kracke F, Wenners J, Jemeljanova A, Kuepper J, Petersen H, Tiller JC. 2015. Nontoxic, hydrophilic cationic polymers—identified as class of antimicrobial polymers. Macromol Biosci 15:1710–1723. https://doi.org/10.1002/mabi.201500207.
52. Tejero R, López D, López-Fabal F, Gómez-Garcés JL, Fernández-García M. 2015. High efficiency antimicrobial thiazolium and triazolium side-chain

polymethacrylates obtained by controlled alkylation of the corresponding azole derivatives. Biomacromolecules 16:1844–1854. https://doi.org/10.1021/acs.biomac.5b00427.
53. Tossi A, Sandri L, Giangaspero A. 2000. Amphipathic, alpha-helical antimicrobial peptides. Biopolymers 55:4–30. https://doi.org/10.1002/1097-0282(2000)55:1<4::AID-BIP30>3.0.CO;2-M.
54. Zhang J, Kissounko DA, Lee SE, Gellman SH, Stahl SS. 2009. Access to poly-β-peptides with functionalized side chains and end groups via controlled ring-opening polymerization of β-lactams. J Am Chem Soc 131:1589–1597. https://doi.org/10.1021/ja8069192.
55. Sherman F, Hicks J. 1987. Methods in yeast genetics: a laboratory course manual. Cold Spring Harbor Laboratory, Cold Spring Harbor, NY.
56. Shimizu K, Keller NP. 2001. Genetic involvement of a cAMP-dependent protein kinase in a G protein signaling pathway regulating morphological and chemical transitions in *Aspergillus nidulans*. Genetics 157:591–600.
57. Arendrup MC, Guinea J, Cuenca-Estrella M, Meletiadis J, Mouton JW, Lagrou K, Howard SJ, the Subcommittee on Antifungal Susceptibility Testing (AFST) of the ESCMID European Committee for Antimicrobial Susceptibility Testing (EUCAST). 2015. EUCAST definitive document E.DEF 9.3. Method for the determination of broth dilution minimum inhibitory concentration for conidia forming moulds. European Committee for Antimicrobial Susceptibility Testing.
58. Lass-Flörl C, Cuenca-Estrella M, Denning DW, Rodriguez-Tudela JL. 2006. Antifungal susceptibility testing in *Aspergillus* spp. according to EUCAST methodology. Med Mycol 44:S319–S325.
59. Bonapace CR, Bosso JA, Friedrich LV, White RL. 2002. Comparison of methods of interpretation of checkerboard synergy testing. Diagn Microbiol Infect Dis 44:363–366. https://doi.org/10.1016/S0732-8893(02)00473-X.
60. Karlsson AJ, Pomerantz WC, Weisblum B, Gellman SH, Palecek SP. 2006. Antifungal activity from 14-helical β-peptides. J Am Chem Soc 128:12630–12631. https://doi.org/10.1021/ja064630y.